Liu *et al. Chem Synth* 2024;4:37
DOI: 10.20517/cs.2023.52

Chemical Synthesis

Research Article

Open Access

Check for updates

Synthesis and intracellular basic protein delivery of a polyanionic flexible organic framework

Yue-Yang Liu[1,*], Yan Wu[1], Peng Guo[1,2], Hui Wang[1], Wei Zhou[1], Dan-Wei Zhang[1], Zhan-Ting Li[1,2,*]

[1]Department of Chemistry, Fudan University, Shanghai 200438, China.
[2]State Key Laboratory of Organometallic Chemistry, Shanghai Institute of Organic Chemistry, Chinese Academy of Sciences, Shanghai 200032, China.

[*]**Correspondence to:** Prof. Zhan-Ting Li, Dr. Yue-Yang Liu, Department of Chemistry, Fudan University, 2205 Songhu Road, Shanghai 200438, China. E-mail: ztli@fudan.edu.cn; 19110220110@fudan.edu.cn

How to cite this article: Liu YY, Wu Y, Guo P, Wang H, Zhou W, Zhang DW, Li ZT. Synthesis and intracellular basic protein delivery of a polyanionic flexible organic framework. *Chem Synth* 2024;4:37. https://dx.doi.org/10.20517/cs.2023.52

Received: 20 Oct 2023 **First Decision:** 15 Apr 2024 **Revised:** 24 May 2024 **Accepted:** 7 Jun 2024 **Published:** 26 Jun 2024

Academic Editor: Guangshan Zhu **Copy Editor:** Pei-Yun Wang **Production Editor:** Pei-Yun Wang

Abstract

Although cationic porous polymers have been widely used for gene and drug delivery, the delivering function of anionic porous polymers has rarely been explored. Herein, we prepare a polyanionic flexible organic framework (pa-FOF) through the quantitative formation of the acylhydrazone bond from a tetraanionic tetraaldehyde and a tetraanionic diacylhydrazine. Pa-FOF is highly water-soluble and has a size of 26 to 51 nm, which depends on the concentration of the monomers, and an aperture of approximately 3.8 nm. Fluorescence, zeta potential, confocal laser scanning microscopic and flow cytometric experiments reveal that pa-FOF can adsorb basic proteins, including lysozyme, trypsin and cytochrome c, which is driven by intermolecular ion-pairing electrostatic attraction and hydrophobicity, and realizes efficient intracellular delivery of the adsorbed proteins. Confocal laser scanning microscopic imaging experiments further illustrate that the delivery of cytochrome c can significantly increase its ability of causing cell apoptosis.

Keywords: Flexible organic framework, polyanionic polymer, basic protein, delivery

INTRODUCTION

Porous polymers have attracted the attention of chemists for several decades owing to their great potential as separation, catalysis, environmental and delivery materials[1-6]. Three-dimensional (3D) polymers are

structurally ideal for generating intrinsic pores. Since the seminal theoretical study by Flory in the 1940s[7], many kinds of 3D polymers have been constructed from flexible multi-armed monomers as biomedical materials[8-13]. In this context, cationic polymers with inherent pores have been extensively used for intracellular delivery of DNA and proteins by utilizing the binding affinity of cationic materials with negatively charged cell membranes to potentiate cellular internalization[14-21]. However, their cytotoxicity and interaction with serum proteins greatly limit their clinical applications[22,23]. Modification on the surface of cationic carriers with anionic polymers, such as hyaluronic acid, can efficiently reduce the toxicity of cationic carriers and simultaneously maintain their capacity in intracellular internalization[24-26]. The efficiency of polymers for protein delivery can also be improved by modifying the surface of polymers through techniques such as fluorination, boronation, or guanidinylation[27]. Components that possess both hydrophobic and hydrophilic have also been revealed to be more conducive to promoting protein delivery. Related to this promotion effect, zwitterionic polymers can exhibit better binding ability to proteins and cell membranes, facilitating protein packaging and intracellular uptake of nanoparticles[28]. Nevertheless, the potential of utilizing anionic polymers for intracellular delivery of biofunctional molecules or drugs has rarely been explored[29].

Since the pioneering research on dynamers by Skene and Lehn[30], dynamic covalent polymers have been widely used for constructing thermodynamically controlled macromolecular and supramolecular targets[31-37]. We have recently constructed a kind of water-soluble flexible organic framework (FOF) through quantitative acylhydrazine or disulfide bond formation[38-43]. These water-soluble polymeric frameworks possess intrinsic nano-scale pores that can include proteins[38], DNA[39], endotoxin[40], porphyrin photodynamic agents[41], and residual neuromuscular blocking agents[42], driven by ion pairing electrostatic attraction and/or hydrophobicity. The polycationic FOFs have been revealed to display hydrodynamic diameters (D_H) ranging from 50 to 120 nm, depending on the monomer concentrations, which enables intracellular delivery of acidic proteins[38]. It is expected that cationic porous polymers cannot efficiently adsorb basic proteins due to intermolecular electrostatic repulsion, while electrostatic attraction may facilitate their adsorption by anionic porous systems, which has not been reported yet. To explore this potential, we have designed and prepared a new acylhydrazone-based polyanionic FOF **pa-FOF**. Here, we report that this porous polyanionic framework can adsorb basic proteins, including lysozyme, trypsin, and cytochrome c, and realize their efficient intracellular delivery.

EXPERIMENTAL

Materials and measurements

All reagents and solvents are commercially available and used as received unless otherwise specified for purification. ^{1}H and ^{13}C nuclear magnetic resonance (NMR) spectra were recorded with an AVANCE III HD 400 MHz spectrometer (Bruker) in the indicated solvents at 25 °C. Ultraviolet (UV)-visible (Vis) spectra were tested by PerkinElmer LAMBDA 650 UV/Vis/near infra-red (NIR) spectrometer. Fourier transform infrared (FTIR) spectroscopic characterization was performed on a Nicolet iS10 FTIR spectrometer (ThermoFisher, USA). Dynamic light scattering (DLS) experiments were tested by Malvern Zetasizer Nano ZS90 using a monochromatic coherent He-Ne laser (633 nm) as the light source and a detector that detected the scattered light at an angle of 90°. The cells were observed by confocal laser scanning microscopy (CLSM) (Zeiss LSM880). Cell viability was measured by Microplate Reader (BioTek Epoch 2). The flow cytometry assay instrument model is a Gallios 3L 10C flow cytometry system (Beckman Coulter, USA). Fluorescein isothiocyanate (FITC), bovine serum albumin (BSA) and trypsin from porcine pancreas were purchased from Macklin. Myoglobin, CytC from equine heart and lysozyme from chicken egg white were purchased from Sigma-Aldrich. Hoechst 33342 and Lyso-Tracker Red (DND-99, Invitrogen) were purchased from Beyotime Biotechnology. Fetal bovine serum (FBS), 1640 medium, 0.25% Tryspin-EDTA (1X) and Penicillin-Streptomycin (5,000 U/mL) were purchased from Thermo Fisher Scientific. Cell

Counting Kit-8 (CCK-8) was purchased from Beyotime Biotechnology. Ana-1 (BNCC338182), H9C2 (BNCC337726) and RAW264.7 (BNCC354753) cell lines were purchased from BeiNa Culture Collection. Michigan Cancer Foundation-7 (MCF-7) cell line was purchased from Shanghai Meixuan Biology Science and Technology. The ^{1}H and ^{13}C NMR spectra of new compounds are provided in Supplementary Materials.

Cell line and cell culture[44]

MCF-7, H9C2, RAW264.7 and ana-1 cells were incubated in 1640 medium with 10% FBS and 1% penicillin-streptomycin at 37 °C in a humidified atmosphere containing 5% CO_2. L02 cells were incubated in 1640 medium with 20% FBS and 1% penicillin-streptomycin at 37 °C. L929 and A549 cells were incubated in Dulbecco's modified Eagle's medium (DMEM) with 10% FBS and 1% penicillin-streptomycin at 37 °C. Before experiments, cells were cultured until they reached confluence.

Synthesis of pa-FOF

The solution containing compound **T1** (375 mg, 0.36 mmol) and **L1** (409 mg, 0.72 mmol) in water (10 mL) was adjusted to pH 6.5 by adding 1 M hydrochloric acid. The resulting solution was further stirred at room temperature for 24 h to afford the solution of **pa-FOF**. ^{1}H NMR in D_2O indicated that the reaction was complete in 24 h, and **T1** and **L1** reacted to yield **pa-FOF** quantitatively.

Synthesis of fluorescent dye-labeled proteins

BSA, myoglobin, lysozyme, cytochrome c and trypsin were dissolved in phosphate-buffered saline (PBS) buffer at pH 7.4. All proteins are fluorescently labeled with FITC at a FITC/protein molar ratio of 3:1. The reaction was carried out in the dark for 24 h at room temperature. After the reaction, the reaction fluid is transferred to a dialysis bag with a molecular weight of 10,000 Da to remove the excess FITC molecules using PBS and water, respectively. The purified products were subsequently lyophilized to yield FITC-labeled proteins: FITC-BSA, FITC-myoglobin, FITC-lysozyme, FITC-cytochrome c, and FITC-trypsin.

Dialysis experiments

The solution containing **pa-FOF** (10 μg/mL) and FITC-lysozyme (8 μg/mL) (1.0 mL) was added to a dialysis bag (cutoff M_n = 50 kDa), immersed in 15 mL of PBS at pH 7.4. Dialysis was performed for 22 h at 37 °C. Subsequently, the fluorescence spectrum of the buffer was recorded, showing no lysozyme fluorescence. Similarly, the fluorescence intensity of the solution in the dialysis bag was also comparable with that of the pre-dialysis fluid.

Cytotoxicity text[44]

The *in vitro* cytotoxicity was assessed using the CCK-8 assay on H9C2, ana-1, L02, L929, and MCF-7 cell lines. Specifically, MCF-7 cells were seeded in 96-well plates at a density of 2×10^4 cells per well and incubated for 24 h at 37 °C in a 5% CO_2 atmosphere. Once the cells adhered, they were treated with **pa-FOF** at concentrations ranging from 0 to 512 μM. For the negative control group, 100 μL of PBS was added per well. After a 24-hour incubation, the medium was replaced with 100 μL of fresh medium containing 10 μL of CCK-8 solution. Then, after incubating for 1 h, absorbance was measured at 450 nm using a microplate reader. Relative cell viability was calculated using: cell viability = [OD450 (samples)/OD450 (control)] × 100%, where OD450 (control) represented the absorbance in the absence of **pa-FOF**, and OD450 (samples) indicated the absorbance in the presence of **pa-FOF**. Each value represents the mean from three independent experiments.

Hemolysis assay[44]

Fresh rats red blood cells (RBCs) and human red blood cells (HBCs) in Alsever's solution were obtained from Guangzhou Hongquan Biological Science and Technology Co., Ltd (Guangzhou, China). These cells were

centrifuged at 2,000 rpm for 10 min. The collected RBCs were then washed with an equal volume of saline to replace the Alsever's solution. Subsequently, 0.63 mL of RBC and HBC suspensions were each incubated separately with 0.07 mL of **pa-FOF** at various concentrations, saline (negative control), and ultrapure water (positive control) at 37 °C for 1 h. After incubation, the mixtures were centrifuged at 3,000 rpm for 10 min. From each sample, 400 μL of the supernatant was transferred into a 96-well plate, and the absorbance at 540 nm was measured using a microplate reader. The hemolysis rate was calculated according to:

$$\text{Hemolysis (\%)} = (A_{sample} - A_{negative}) / (A_{positive} - A_{negative}) \times 100\%$$

Where A_{sample} represents the absorbance of the test samples. $A_{positive}$ and $A_{negative}$ denote the absorbance of the positive control and negative control, respectively.

CLSM[44]

For CLSM observations, ana-1 cells (1×10^5 cells per dish) were seeded in coverglass bottom dishes (35 mm × 35 mm). After culture for 24 h, the cells were incubated with DMEM/F12 medium containing FITC-lysozyme, FITC-cytochrome c, FITC-trypsin, FITC-lysozyme + **pa-FOF** ([FITC-lysozyme] = 12 μg/mL; [**pa-FOF**] = 0-18 μg/mL), FITC-cytochrome c + **pa-FOF** ([FITC-cytochrome c] = 12 μg/mL; [**pa-FOF**] = 0-18 μg/mL), FITC-trypsin + **pa-FOF** ([FITC-trypsin] = 12 μg/mL; [**pa-FOF**] = 0-12 μg/mL) for 16 h at 37 °C. After washing the cells by PBS twice to remove excessive **pa-FOF** and proteins, the cells were treated with 1 μg/mL Hoechst 33342 for 10 min and 75 nmol/L Lyso-Tracker Red for 1 h at 37 °C and then washed with PBS three times. The cells were imaged on CLSM on Zeiss LSM880.

For detection of apoptosis after treated with **pa-FOF** and cytochrome c, the supernatant of the treated cells (which contain floating apoptotic cells) was incubated with propidium iodide (PI, 50 μg/mL), followed by nuclear staining with Hoechst 33342.

Flow cytometry assay[38]

Ana-1 cells were seeded at 1×10^6 cells per well in a 12-well plate and further cultured for 24 h in a DMEM/F12 medium. Free FITC-lysozyme, FITC-lysozyme + **pa-FOF** ([FITC-lysozyme] = 12 μg/mL; [**pa-FOF**] = 0-20 μg/mL) were added to the cells, respectively. After incubating for 16 h, the semi-adherent cells were detached using 0.5 mL PBS and analyzed by flow cytometry in the FL1 or FL3 channel using a flow cytometry system.

Cellular uptake mechanism study[38]

Ana-1 cells were seeded at a density of 1×10^6 cells per well in a 12-well plate and further cultured for an additional 24 h. Then, the cells were incubated with 0.5 mL culture medium containing dynasore (100 μM), chlorpromazine (3 μg/mL), Nystatin (15 μg/mL), amiloride (3 mM), and β-CD (0.5 mM) at 37 °C for 1 h, respectively. The solution of FITC-lysozyme + **pa-FOF** ([FITC-lysozyme] = 12 μg/mL; [**pa-FOF**] = 9 μg/mL) was then added in the dishes and the cells were incubated at 37 °C for another 16 h. At the end of the experiment, the cells were harvested for flow cytometry assay.

RESULTS AND DISCUSSION

Synthesis and characterization of pa-FOF

Previous work confirmed that multi-armed acylhydrazines and aldehydes can react quantitatively to form acylhydrazone in water under weak acid conditions[38]. We, thus, prepared preorganized tetracationic tetraaldehyde **T1** and biacylhydrazines **L1** to build a new water-soluble porous framework [Scheme 1]. For the synthesis of **T1**, compound **1** first reacted with tetrabromide **2** to produce tetraaldehyde **3** in a 67% yield. Treatment of **3** with LiOH in water and tetrahydrofuran afforded **T1** in an 85% yield. For the preparation of

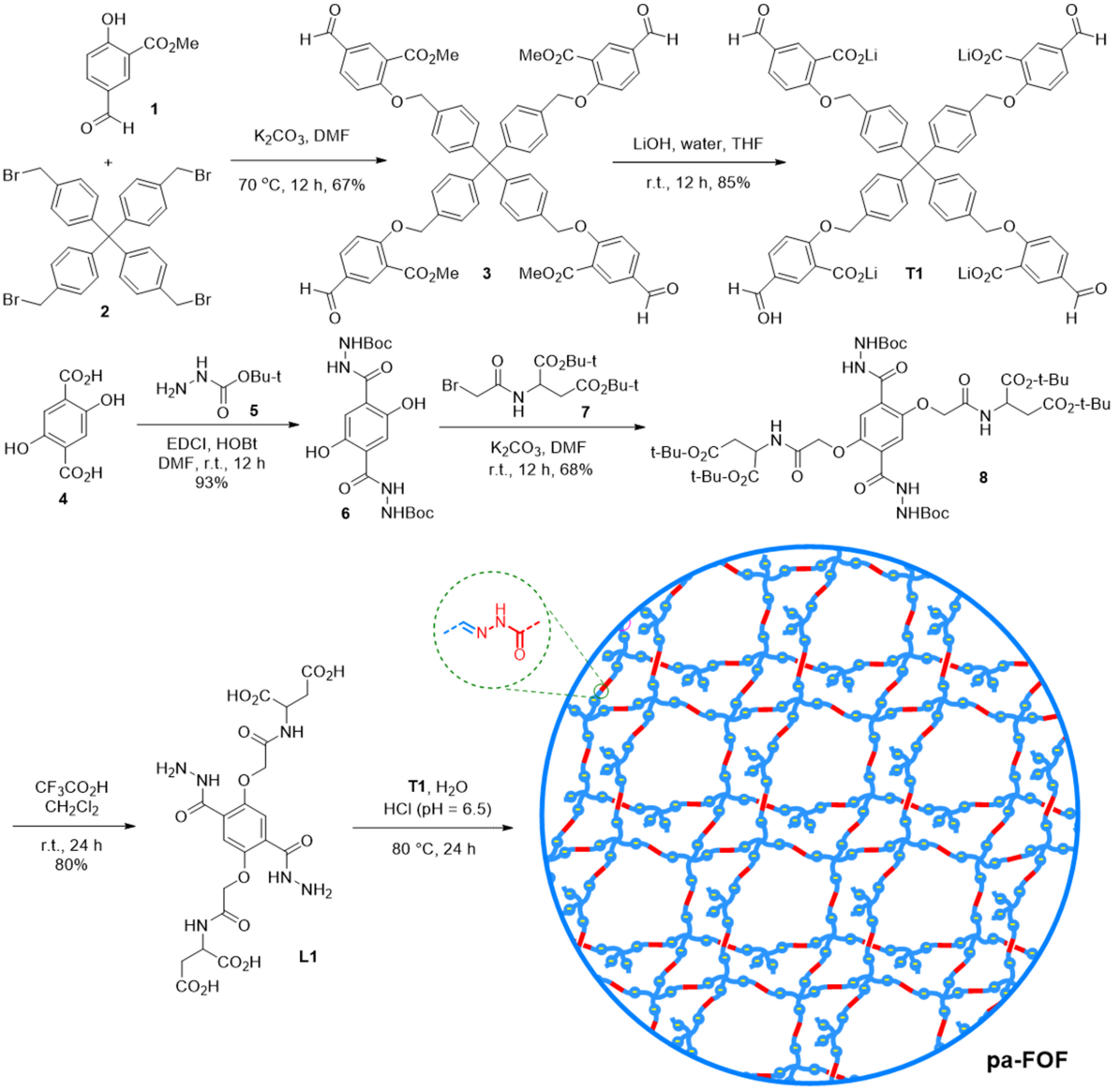

Scheme 1. The synthesis of **pa-FOF**. Pa-FOF: Polyanionic flexible organic framework.

L1, compound **4** was first coupled with **5** to produce **6** in a 93% yield. Treating **6** with bromide **7**[45] with potassium carbonate as a base to afford compound **8** in a 68% yield. This intermediate was treated with trifluoroacetic acid to obtain diacylhydrazine **L1** in an 80% yield. The 1:2 mixture of **T1** and **L1** in dilute hydrochloric acid was stirred at 80 °C for 24 h to afford the porous framework **pa-FOF**. The ^{1}H NMR spectrum of their 1:2 mixture ([**T1**] = 5.0 mM) in D_2O showed that, after 24 h at 80 °C, the diagnostic signal of the O=C*H* group of **T1** at 9.7 ppm disappeared completely [Supplementary Figure 1]. The ^{1}H NMR spectra of the resulting products were all considerably broad, suggesting the formation of hydrazone-based polymeric species. The solution gave a comparable spectrum after standing at room temperature for 12 days, supporting that the resulting framework was stable.

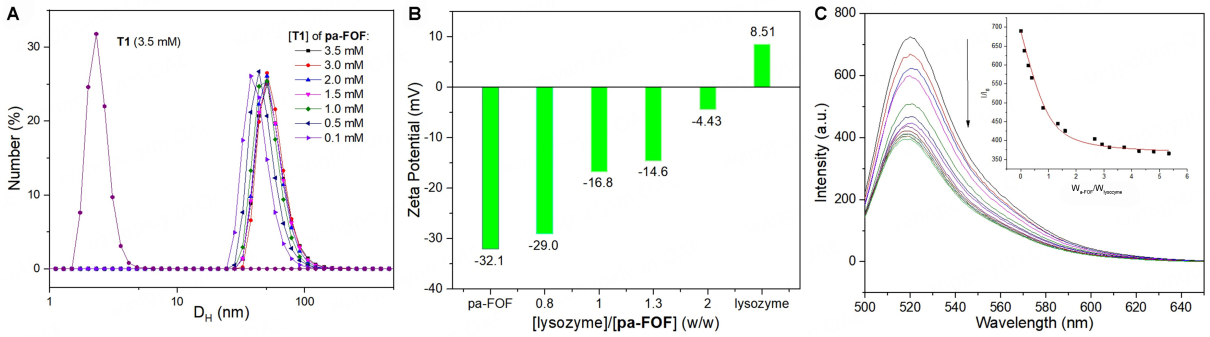

Figure 1. (A) DLS profile of **T1** and **pa-FOF** of different concentrations in water; (B) Zeta potential of **pa-FOF** (10 μg/mL), lysozyme (8 μg/mL) and their mixtures of varying ratios; (C) Fluorescence spectra (λ_{ex} = 490 nm) of FITC-lysozyme (7 μM) in the presence of the increasing amount of **pa-FOF** ([**T1**] = 0-36 μM) in water [Inset: I/I_0 *vs.* $W_{pa\text{-}FOF}/W_{lysozyme}$ (λ_{em} = 520 nm)]. DLS: Dynamic light scattering; pa-FOF: polyanionic flexible organic framework; FITC: fluorescein isothiocyanate.

DLS experiments of the solution of **pa-FOF** revealed a D_H of 51 nm at [**T1**] = 3.5 mM. The D_H value decreased with the concentration, but even at [**T1**] = 0.1 mM, it still reached 26 nm [Figure 1]. Comparable results could be obtained after the solutions were left at room temperature for one week [Supplementary Figure 2], which supported its high stability. In contrast, the solution of **T1** afforded a D_H value of 2.3 nm, consistent with its size as a single molecule. Molecular modeling revealed that, by assuming that the condensation reaction to form the acylhydrazone bond is an ideal process and linkers that connect the tetraphenylmethane nodes are completely stretched, **pa-FOF** would form a dynamic 3D diamondoid framework, with the aperture calculated to be 3.8 nm [Supplementary Figure 3].

Adsorption of pa-FOF for lysozyme

Lysozyme is a positively charged protein that has an isoelectric point of 10.6 to 10.9 and a dimension of 3 nm × 3 nm × 4.5 nm. Thus, we first studied the adsorption of **pa-FOF** for lysozyme. At 8 μg/mL, lysozyme has a zeta potential of +8.51 mV, while the zeta potential of **pa-FOF** at 10 μg/mL was determined to be -32.1 mV, well reflecting the negative surface character of the framework. Adding lysozyme to the solution of **pa-FOF** caused a continuous decrease of the zeta potential [Figure 1B]. However, even with the addition of two equivalents of lysozyme, the zeta potential remained negative (-4.43 mV). These results suggested that **pa-FOF** could adsorb lysozyme to its interior. If the adsorption of lysozyme to the surface of **pa-FOF** was the main interaction mechanism, it would cause the overturn of the zeta potential to positive values[38]. Dialysis experiments using a dialysis membrane with cutoff M_n of 50 kDa also showed that **pa-FOF** (10 μg/mL) could prevent the dialysis of FITC-lysozyme (8 μg/mL), which further supported the inclusion and retainment of the protein by **pa-FOF**. The apparent binding constant, defined for the 1:1 complexation between the **T1** unit of **pa-FOF**, and lysozyme, was then determined to be 6.0×10^5 M^{-1} using fluorescence titration experiments by adding **pa-FOF** to the solution of FITC-labeled lysozyme [Figure 1C][38]. Using the same method, we determined the apparent binding constant between **pa-FOF** and myoglobin, which has an isoelectric point of 7.07, to be 7.15×10^3 M^{-1} [Supplementary Figure 4A]. In contrast, acidic BSA, which has an isoelectric point of 4.7, was not adsorbed by **pa-FOF**, since adding the polymeric framework to its solution did not cause observable change of its fluorescence [Supplementary Figure 4B]. These results showed that the adsorption of **pa-FOF** for lysozyme should be driven by both intermolecular electrostatic attraction and hydrophobicity.

Intracellular delivery of basic proteins by pa-FOF

The ability of **pa-FOF** for intracellular delivery of FITC-lysozyme was first studied. For this aim, we first chose the ana-1 cell line by staining the nuclei and lysosomes with Hoechst 33342 and Lyso-Tracker Red. In

order to determine the optimal concentration of FITC-lysozyme, the cells were subjected to CLSM after incubation with FITC-lysozyme (4, 8, and 12 μg/mL) and **pa-FOF** (12 μg/mL) for 16 h. It can be found that for the sample prepared with FITC-lysozyme of 12 μg/mL, the fluorescence intensity varied most after **pa-FOF** was added and highly colocalized with lysosomes stained with Lyso-Tracker Red [Supplementary Figure 5]. Since in neutral media, **pa-FOF** could include and retain FITC-lysozymes, it is rational to propose that this release took place due to the internal acidity of lysosomes which caused the hydrolysis of the hydrazone bonds and decomposition of **pa-FOF**. The colocalization analysis for ana-1 cells, which were treated with FITC-lysozyme (12 μg/mL) and **pa-FOF** (12 μg/mL) for 16 h, between the signal of the protein and lysotracker afforded the Pearson's correlation coefficient of 0.75 [Supplementary Figure 6], indicating that the delivery of **pa-FOF** enhanced the targeting of FITC-lysozyme lysosomes. Therefore, subsequent experiments were conducted with the concentration of FITC-lysozyme kept at 12 μg/mL. The delivering ability of **pa-FOF** for FITC-lysozyme was then evaluated. CLSM studies showed that adding **pa-FOF** continuously increased the fluorescence intensity of FITC-lysozyme [Figure 2], supporting its delivering ability for the protein. At the concentration of 9 μg/mL, **pa-FOF** could cause 19 times the fluorescence intensity increase of FITC-lysozyme in ana-1 cells [Supplementary Figure 7]. Further increasing the concentration of **pa-FOF** to 18 μg/mL did not further enhance the fluorescence intensity, indicating that **pa-FOF** of 9 μg/mL already adsorbed FITC-lysozyme completely. Further CLSM experiments revealed that **pa-FOF** could also deliver lysozyme into other cells, such as L929 and RAW264.7 cells, and cancer cells, such as MCF-7 and A549 cells [Supplementary Figure 8]. Moreover, CLSM experiments also showed that other basic proteins, including trypsin and cytochrome c with an isoelectric point of 11 or 9.5, could also be transported by **pa-FOF** into ana-1 cells [Supplementary Figures 9 and 10].

Flow cytometric experiments were then conducted to quantitatively evaluate the delivery of FITC-lysozyme by **pa-FOF** into ana-1 cells [Figure 3]. In the absence of **pa-FOF**, the percentage of transfected cells was determined to be 14%, reflecting that basic lysozyme has moderate electrostatic interaction with the negatively charged surface of the cells, facilitating its endocytosis. With the delivery of **pa-FOF** of 6.0, 9.0, 12 and 15 μg/mL, the percentage of transfected cells increased to 61%, 72%, 78% and 82%, respectively. Since the above results confirmed that lysozyme was included into the interior of **pa-FOF**, these substantially increased transfections supported that **pa-FOF** possesses important delivering ability.

Mechanisms underlying pa-FOF-mediated protein uptake

Cationic porous frameworks have been established to enter cells by facilitating interactions with inherently negatively charged cellular membranes. For nano-scaled anionic porous polymers, this process may be driven by hydrophobicity between their surfaces followed by endocytosis. To get insight into the transmembrane process of protein-included **pa-FOF**, we performed several intracellular experiments in the presence of a panel of inhibitors that inhibit different intracellular internalization pathways[46]. **pa-FOF** displayed moderate fluorescence, which was used to evaluate its uptake by ana-1 cells after incubating for 16 h. The fluorescence of **pa-FOF** (blue) could be clearly observed in the cell [Supplementary Figure 11], proving that **pa-FOF** entered the cell. Stepwise incubation experiments were also conducted to test the delivering efficiency of **pa-FOF**. To do this, **pa-FOF** (12 μg/mL) was first incubated with ana-1 cells for 16 h. Then, FITC-lysozyme (12 μg/mL) was added, and incubation was continued for another 16 h. CLSM imaging showed that the fluorescence intensity of FITC-lysozyme in the ana-1 cells was much weaker than that of the above samples obtained by co-incubation of **pa-FOF** and FITC-lysozyme of the identical concentration [Figure 4], further confirming the delivering function of **pa-FOF** for lysozyme. We further conducted CLSM and flow cytometric experiments for the solution of **pa-FOF** and FITC-myoglobin [Supplementary Figures 12 and 13], which showed that **pa-FOF** could also encapsulate and deliver the protein. Since myoglobin has an isoelectric point of 7.07, it is reasonable to propose that this encapsulation and delivery should be driven mainly by hydrophobic interaction and weak electrostatic interaction.

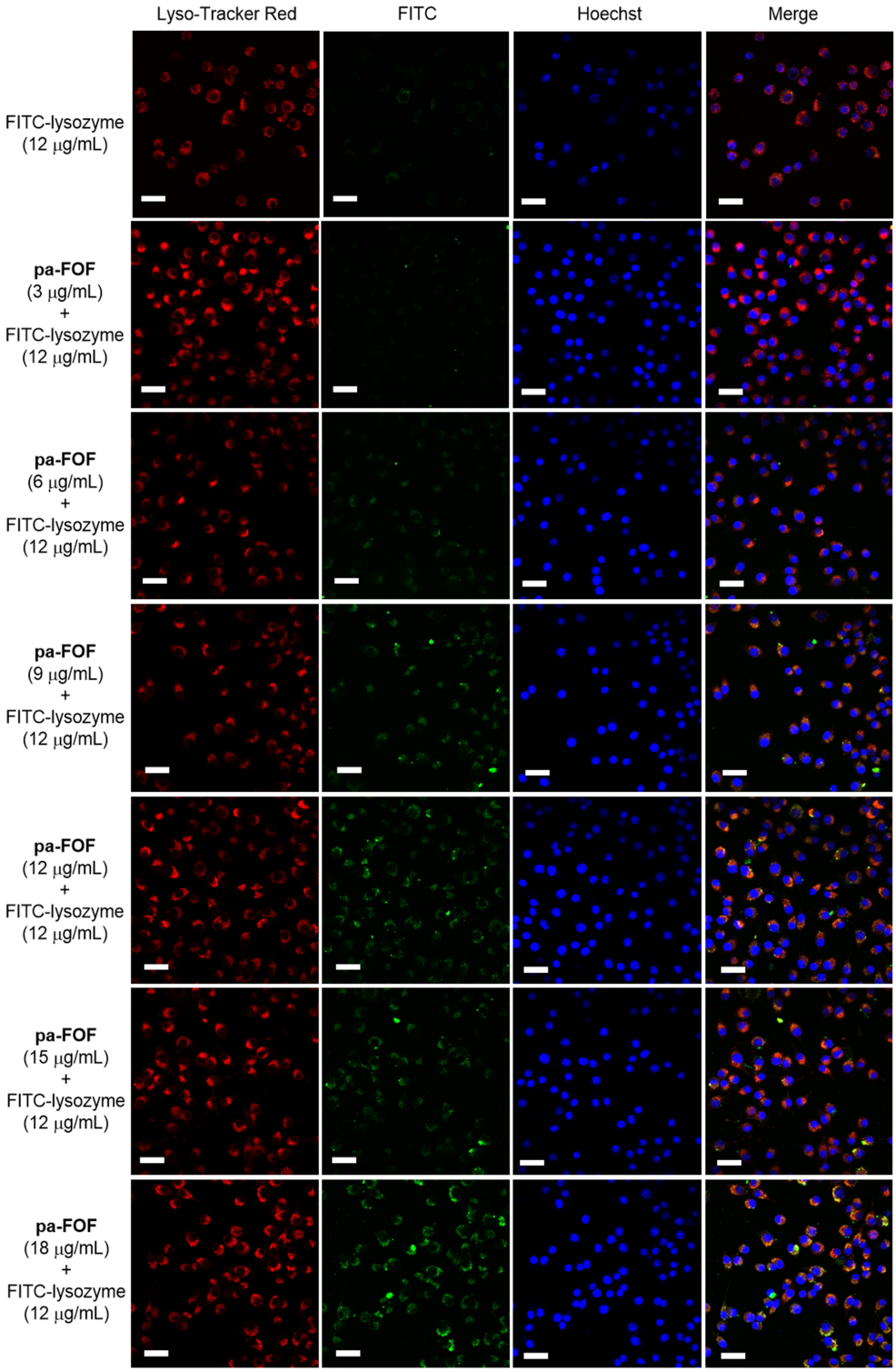

Figure 2. CLSM images of ana-1 cells after incubation for 16 h with FITC-lysozyme (12 μg/mL) in the presence of **pa-FOF** (0-18 μg/mL). The lysosomes and nuclei were stained with Lyso-Tracker Red (red) and Hoechst 33342 (blue), respectively. Scale bar: 20 μm. CLSM: confocal laser scanning microscopy; FITC: fluorescein isothiocyanate; pa-FOF: polyanionic flexible organic framework.

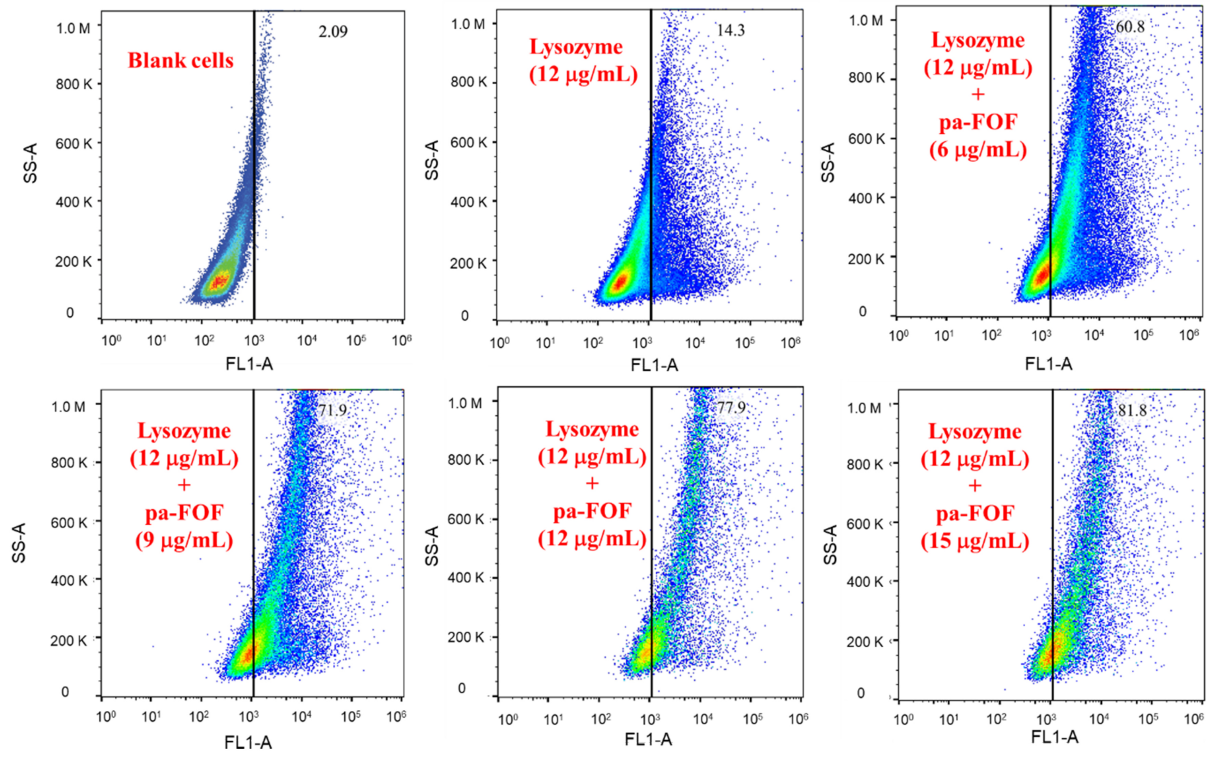

Figure 3. Flow cytometric experiments for the delivery of FITC-lysozyme (12 μg/mL) into ana-1 cell lines by **pa-FOF** (0-15 μg/mL). The cells were tested after incubation in an F12/DMEM medium at 37 °C for 16 h. FITC: Fluorescein isothiocyanate; pa-FOF: polyanionic flexible organic framework; DMEM: Dulbecco's modified Eagle's medium.

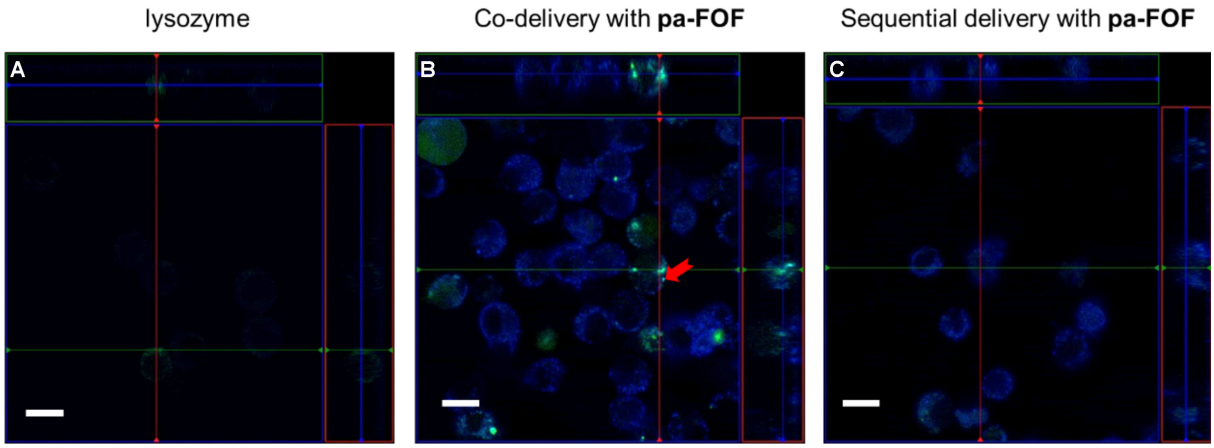

Figure 4. CLSM images of lysozyme (12 μg/mL) in ana-1 cells. (A) incubation alone for 16 h; (B) incubation simultaneously with **pa-FOF** (12 μg/mL) for 16 h; and (C) incubation for 16 h with **pa-FOF** (12 μg/mL) after **pa-FOF** was incubated with ana-1 cells for 16 h. Scale bar: 20 μm. CLSM: Confocal laser scanning microscopy; pa-FOF: polyanionic flexible organic framework.

We then studied the inhibition effect of endocytosis inhibitors, including chlorpromazine and dynosore which inhibit clathrin-mediated endocytosis, nystatin which inhibits caveolae-mediated endocytosis, amiloride which inhibits micropinocytosis, and β-CD which inhibits lipid raft-mediated endocytosis, for the delivery of **pa-FOF** for FITC-lysozyme[47]. For doing these, ana-1 cells were pretreated with the endocytosis inhibitors, and then **pa-FOF** and FITC-lysozyme were incubated with the cells for 16 h. The counts of

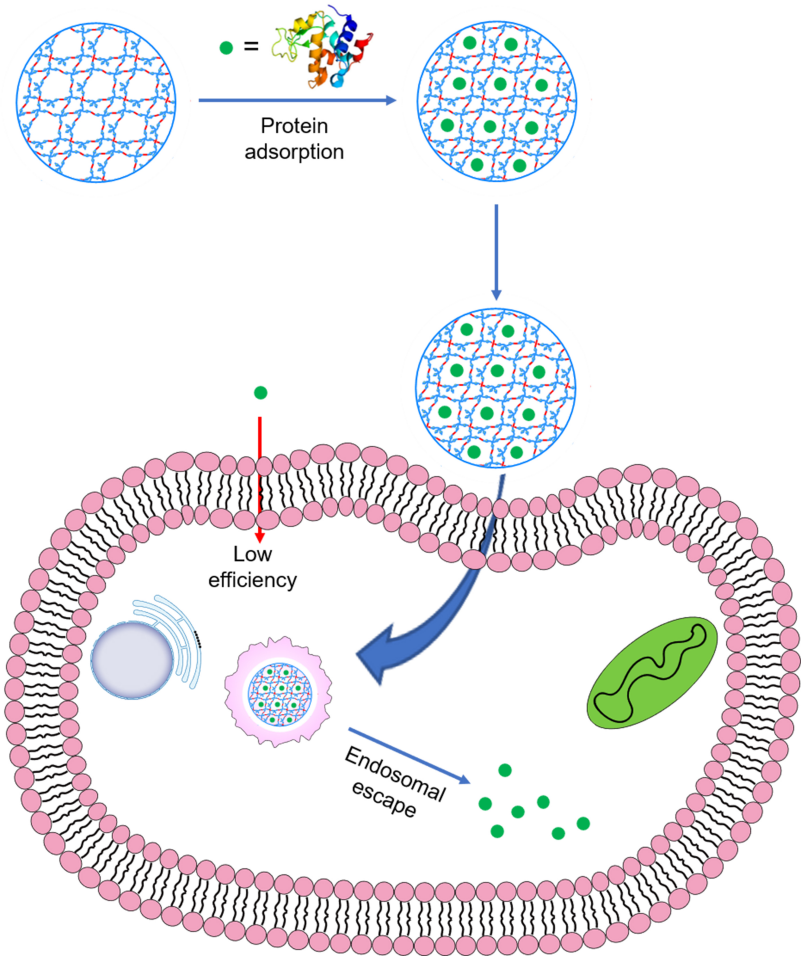

Figure 5. The endocytosis mechanism of **pa-FOF** for intracellular transport of basic proteins. pa-FOF: Polyanionic flexible organic framework.

positive cells were gained for these pretreated cells and, for comparison, untreated ana-1 cells [Supplementary Figure 14]. It can be found that, except that dynosore did not impose observable inhibition, amiloride, chlorpromazine, nystatin and β-CD reduced the delivering ability of **pa-FOF** by 45.9%, 22.7%, 60% and 57.8%, respectively. These results indicated that the delivery of **pa-FOF** for the basic proteins proceeds through different endocytosis pathways [Figure 5].

Increased activity of delivered cytochrome c for inducing cell apoptosis

Cytochrome c, a basic mitochondrial protein, has been well-known as a key mediator of apoptosis[48]. In addition to endogenous release from mitochondria to cytoplasm to cause cell apoptosis, exogenous delivery of cytochrome c into cellular cytoplasm also promotes this process[49]. Therefore, we further studied the promoting effect of **pa-FOF**-mediated intracellular delivery of cytochrome c for ana-1 cell apoptosis. CLSM imaging experiments revealed that **pa-FOF** alone could not induce the apoptosis of ana-1 cells. However, its delivery significantly enhanced the apoptotic effect of FITC-cytochrome c [Figure 6].

CLSM experiments revealed that ana-1 cells that were not treated and incubated with **pa-FOF** were more consistent in size. The cell membranes were intact; there were no obvious protrusions on the surface, and fluorescence staining was uniform, whereas cells treated with **pa-FOF** and cytochrome c were

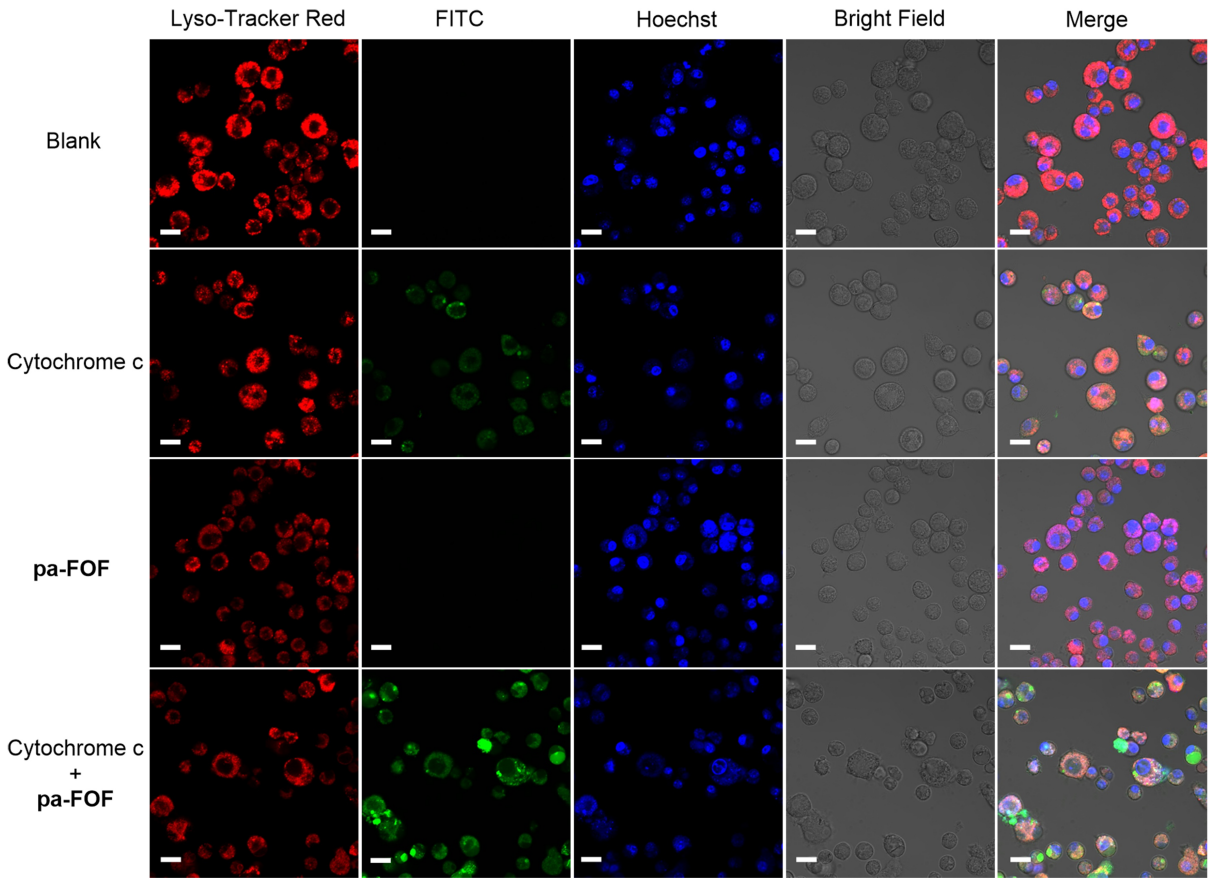

Figure 6. CLSM images of ana-1 cells after incubation for 16 h with FITC-cytochrome c (5 μg/mL), **pa-FOF** (12 μg/mL), and FITC-cytochrome c (5 μg/mL)/**pa-FOF** (12 μg/mL). The lysosomes and nuclei were stained with Lyso-Tracker Red (red) and Hoechst 33342 (blue), respectively. Scale bar: 20 μm. CLSM: Confocal laser scanning microscopy; FITC: fluorescein isothiocyanate; pa-FOF: polyanionic flexible organic framework.

morphologically irregular, with buds on the cell surface and dendritic irregular protrusions. Similar results were also observed for L929 cells [Supplementary Figure 15]. Apoptotic cells undergo chromatin condensation, which allows the dye to bind to DNA more efficiently. The *p*-glycoprotein on the membrane of apoptotic cells is impaired and does not efficiently exclude Hoechst 33342 from the cell, which increased intracellular accumulation of Hoechst 33342, leading to significant fluorescence enhancement in apoptotic cells than normal cells [Supplementary Figure 16]. These results also supported that, after being encapsulated by **pa-FOF**, the dye-labeled cytochrome c maintained its 3D conformation and, thus, its bioactivity.

Biocompatibility of pa-FOF *in vitro*

Finally, we evaluated the biocompatibility of **pa-FOF**. Its cytotoxicity was assessed in normal cell lines, including H9C2, L02, ana-1, and L929 cells, along with MCF-7 cancer cells using the CCK-8 assay [Figure 7A and B, Supplementary Figure 17]. The results showed that within the concentration range of 512 μg/mL for **pa-FOF**, all the cells had a survival rate of > 70%. Hemolysis tests with rats RBC and HBC revealed that **pa-FOF** displayed low hemolysis activity. In the presence of 512 μg/mL for **pa-FOF**, the hemolysis ratios of the cells remained as low as < 5% [Figure 7C and D].

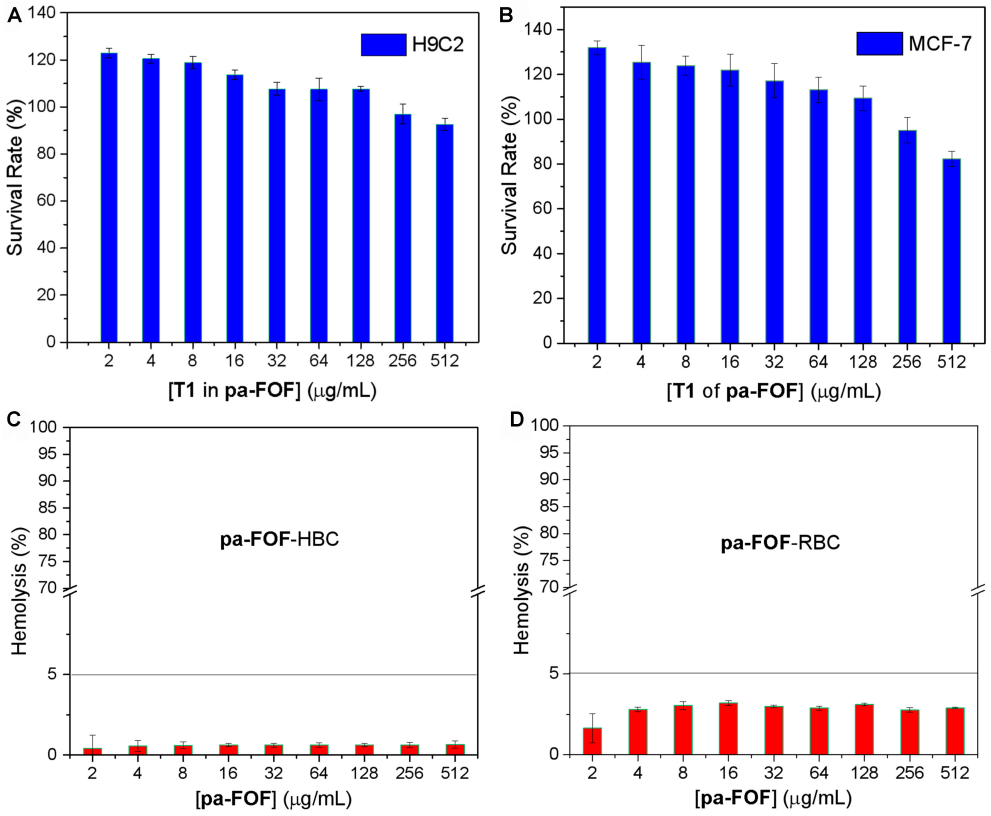

Figure 7. Cell viability values (%) of (A) H9C2 and (B) MCF-7 cell lines assessed by CCK-8 proliferation tests versus incubation concentration of **pa-FOF** represented by [**T1**]. The cells (~2 × 10^4 per well) were incubated with the **pa-FOF** at 37 °C for 24 h. Error bars represent the s.d. of uncertainty for each point. Hemolysis rates of **pa-FOF** in (C) human and (D) rats red blood cells. MCF-7: Michigan Cancer Foundation-7; CCK-8: Cell Counting Kit-8; pa-FOF: polyanionic flexible organic framework.

CONCLUSION

We demonstrate that **pa-FOF** can adsorb basic proteins, driven by intermolecular electrostatic attraction and hydrophobicity. The FOF has a nano-scale size and enables intracellular delivery of the adsorbed proteins. The delivery of cytochrome c significantly increases its ability of causing apoptosis, which reversely supports the delivering ability of the FOF. The internalization of the **pa-FOF** into cells opens the possibility of utilizing this kind of intrinsically porous polymer for delivering cationic drugs. Thus, in the future, systems with varying charge densities and pore sizes will be constructed for this purpose and for exploring their confinement effect for modulating the activity of adsorbed proteins.

DECLARATIONS

Authors' contributions

Conceptualization: Liu YY, Zhou W, Zhang DW, Li ZT

Conducted the synthesis, characterization, calculation and measurements: Guo P, Wu Y, Liu YY, Wang H

Data analysis and original draft: Liu YY

Resources: Wang H, Zhou W, Zhang DW, Li ZT

Review and writing finalization: Li ZT

Availability of data and materials

The experimental data and associated test results are published as Supplementary Materials in the journal.

Financial support and sponsorship

We are grateful to the National Natural Science Foundation of China (NSFC) for financial support (21890730, 21890732 and 21921003).

Conflicts of interest

All authors declared that there are no conflicts of interest.

Ethical approval and consent to participate

Cell experiments were performed in accordance with the guidelines of the Animal Care and Use Committee of Fudan University (2022JS-Department of Chemistry-012).

Consent for publication

Not applicable.

REFERENCES

1. Wu D, Xu F, Sun B, Fu R, He H, Matyjaszewski K. Design and preparation of porous polymers. *Chem Rev* 2012;112:3959-4015. DOI PubMed
2. Wu J, Xu F, Li S, et al. Porous polymers as multifunctional material platforms toward task-specific applications. *Adv Mater* 2019;31:e1802922. DOI PubMed
3. Ji W, Wang T, Ding X, Lei S, Han B. Porphyrin- and phthalocyanine-based porous organic polymers: from synthesis to application. *Coord Chem Rev* 2021;439:213875. DOI
4. Chen W, Chen P, Zhang G, et al. Macrocycle-derived hierarchical porous organic polymers: synthesis and applications. *Chem Soc Rev* 2021;50:11684-714. DOI PubMed
5. Zhang Z, Jia J, Zhi Y, Ma S, Liu X. Porous organic polymers for light-driven organic transformations. *Chem Soc Rev* 2022;51:2444-90. DOI PubMed
6. Yu SB, Lin F, Tian J, Yu J, Zhang DW, Li ZT. Water-soluble and dispersible porous organic polymers: preparation, functions and applications. *Chem Soc Rev* 2022;51:434-49. DOI PubMed
7. Flory PJ. Molecular size distribution in three dimensional polymers. I. gelation[1]. *J Am Chem Soc* 1941;63:3083-90. DOI
8. Kopeček J, Yang J. Hydrogels as smart biomaterials. *Polym Int* 2007;56:1078-98. DOI
9. Wang W, Narain R, Zeng H. Rational design of self-healing tough hydrogels: a mini review. *Front Chem* 2018;6:497. DOI PubMed PMC
10. Zheng C, Zhu J, Yang C, Lu C, Chen Z, Zhuang X. The art of two-dimensional soft nanomaterials. *Sci China Chem* 2019;62:1145-93. DOI
11. Xu Z, Chu X, Wang Y, Zhang H, Yang W. Three-dimensional polymer networks for solid-state electrochemical energy storage. *Chem Eng J* 2020;391:123548. DOI
12. Zhu Y, Xu P, Zhang X, Wu D. Emerging porous organic polymers for biomedical applications. *Chem Soc Rev* 2022;51:1377-414. DOI PubMed
13. Tian J, Lin F, Yu S, Yu J, Tang Q, Li Z. Water-dispersible and soluble porous organic polymers for biomedical applications. *Aggregate* 2022;3:e187. DOI
14. Moulton SE, Wallace GG. 3-dimensional (3D) fabricated polymer based drug delivery systems. *J Control Release* 2014;193:27-34. DOI PubMed
15. Asayama S. Molecular design of polymer-based carriers for plasmid DNA delivery *in vitro* and *in vivo*. *Chem Lett* 2020;49:1-9. DOI
16. Zhang M, Hong Y, Chen W, Wang C. Polymers for DNA vaccine delivery. *ACS Biomater Sci Eng* 2017;3:108-25. DOI
17. Cheng Y. Design of polymers for intracellular protein and peptide delivery. *Chin J Chem* 2021;39:1443-9. DOI
18. Calori IR, Braga G, de Jesus PDCC, Bi H, Tedesco AC. Polymer scaffolds as drug delivery systems. *Eur Polym J* 2020;129:109621. DOI
19. Singh N, Son S, An J, et al. Nanoscale porous organic polymers for drug delivery and advanced cancer theranostics. *Chem Soc Rev* 2021;50:12883-96. DOI PubMed

20. Tang Y, Varyambath A, Ding Y, et al. Porous organic polymers for drug delivery: hierarchical pore structures, variable morphologies, and biological properties. *Biomater Sci* 2022;10:5369-90. DOI PubMed
21. Huang P, Deng H, Zhou Y, Chen X. The roles of polymers in mRNA delivery. *Matter* 2022;5:1670-99. DOI
22. Lv H, Zhang S, Wang B, Cui S, Yan J. Toxicity of cationic lipids and cationic polymers in gene delivery. *J Control Release* 2006;114:100-9. DOI PubMed
23. Warga E, Austin-carter B, Comolli N, Elmer J. Nonviral vehicles for gene delivery. *Nano LIFE* 2021;11:2130002. DOI
24. Schlegel A, Largeau C, Bigey P, et al. Anionic polymers for decreased toxicity and enhanced in vivo delivery of siRNA complexed with cationic liposomes. *J Control Release* 2011;152:393-401. DOI PubMed
25. Sun Q, Kang Z, Xue L, et al. A collaborative assembly strategy for tumor-targeted siRNA delivery. *J Am Chem Soc* 2015;137:6000-10. DOI PubMed
26. Richter F, Leer K, Martin L, et al. The impact of anionic polymers on gene delivery: how composition and assembly help evading the toxicity-efficiency dilemma. *J Nanobiotechnology* 2021;19:292. DOI PubMed PMC
27. Zhang Y, Shi J, Ma B, et al. Functionalization of polymers for intracellular protein delivery. *Prog Polym Sci* 2023;146:101751. DOI
28. Zhang Y, Shi J, Ma B, et al. Phosphocholine-functionalized zwitterionic highly branched poly(β-amino ester)s for cytoplasmic protein delivery. *ACS Macro Lett* 2023;12:626-31. DOI PubMed
29. Jakki SL, Ramesh YV, Gowthamarajan K, et al. Novel anionic polymer as a carrier for CNS delivery of anti-Alzheimer drug. *Drug Deliv* 2016;23:3471-9. DOI PubMed
30. Skene WG, Lehn JM. Dynamers: polyacylhydrazone reversible covalent polymers, component exchange, and constitutional diversity. *Proc Natl Acad Sci U S A* 2004;101:8270-5. DOI PubMed PMC
31. García F, Smulders MM. Dynamic covalent polymers. *J Polym Sci A Polym Chem* 2016;54:3551-77. DOI PubMed PMC
32. Ji S, Xia J, Xu H. Dynamic chemistry of selenium: Se-N and Se-Se dynamic covalent bonds in polymeric systems. *ACS Macro Lett* 2016;5:78-82. DOI PubMed
33. Apostolides DE, Patrickios CS. Dynamic covalent polymer hydrogels and organogels crosslinked through acylhydrazone bonds: synthesis, characterization and applications. *Polymer International* 2018;67:627-49. DOI
34. Su D, Coste M, Diaconu A, Barboiu M, Ulrich S. Cationic dynamic covalent polymers for gene transfection. *J Mater Chem B* 2020;8:9385-403. DOI PubMed
35. Zhang Y, Qi Y, Ulrich S, Barboiu M, Ramström O. Dynamic covalent polymers for biomedical applications. *Mater Chem Front* 2020;4:489-506. DOI PubMed PMC
36. Zheng N, Xu Y, Zhao Q, Xie T. Dynamic covalent polymer networks: a molecular platform for designing functions beyond chemical recycling and self-healing. *Chem Rev* 2021;121:1716-45. DOI PubMed
37. Liu W, Yang S, Huang L, Xu J, Zhao N. Dynamic covalent polymers enabled by reversible isocyanate chemistry. *Chem Commun* 2022;58:12399-417. DOI PubMed
38. Lin JL, Wang ZK, Xu ZY, et al. Water-soluble flexible organic frameworks that include and deliver proteins. *J Am Chem Soc* 2020;142:3577-82. DOI PubMed
39. Wang Z, Lin J, Zhang Y, et al. Synthesis and short DNA *in situ* loading and delivery of 4 nm-aperture flexible organic frameworks. *Mater Chem Front* 2021;5:869-75. DOI
40. Sun JD, Li Q, Haoyang WW, et al. Adsorption-based detoxification of endotoxins by porous flexible organic frameworks. *Mol Pharm* 2022;19:953-62. DOI PubMed
41. Xu ZY, Liu HK, Wu Y, et al. Flexible organic framework-based anthracycline prodrugs for enhanced tumor growth inhibition. *ACS Appl Bio Mater* 2021;4:4591-7. DOI PubMed
42. Wu Y, Liu YY, Liu HK, et al. Flexible organic frameworks sequester neuromuscular blocking agents in vitro and reverse neuromuscular block *in vivo*. *Chem Sci* 2022;13:9243-8. DOI PubMed PMC
43. Li Q, Sun J, Yang B, et al. Cucurbit[7]uril-threaded flexible organic frameworks: quantitative polycatenation through dynamic covalent chemistry. *Chin Chem Lett* 2022;33:1988-92. DOI
44. Liu YY, Wang ZK, Yu SB, et al. Conjugating aldoxorubicin to supramolecular organic frameworks: polymeric prodrugs with enhanced therapeutic efficacy and safety. *J Mater Chem B* 2022;10:4163-71. DOI PubMed
45. Jacques V, Dumas S, Sun WC, Troughton JS, Greenfield MT, Caravan P. High-relaxivity magnetic resonance imaging contrast agents. Part 2. Optimization of inner- and second-sphere relaxivity. *Invest Radiol* 2010;45:613-24. DOI PubMed PMC
46. Evans BC, Fletcher RB, Kilchrist KV, et al. An anionic, endosome-escaping polymer to potentiate intracellular delivery of cationic peptides, biomacromolecules, and nanoparticles. *Nat Commun* 2019;10:5012. DOI PubMed PMC
47. Rennick JJ, Johnston APR, Parton RG. Key principles and methods for studying the endocytosis of biological and nanoparticle therapeutics. *Nat Nanotechnol* 2021;16:266-76. DOI PubMed
48. Jiang X, Wang X. Cytochrome C-mediated apoptosis. *Annu Rev Biochem* 2004;73:87-106. DOI PubMed
49. Santra S, Kaittanis C, Perez JM. Cytochrome C encapsulating theranostic nanoparticles: a novel bifunctional system for targeted delivery of therapeutic membrane-impermeable proteins to tumors and imaging of cancer therapy. *Mol Pharm* 2010;7:1209-22. DOI PubMed PMC